Inorg. Chem. **2004**, *43*, 6531–6533

Synthesis and Magnetic Properties of Wheel-Shaped [Mn_{12}] and [Fe_6] Complexes

Evan M. Rumberger, Lev N. Zakharov, Arnold L. Rheingold, and David N. Hendrickson*

Department of Chemistry and Biochemistry, University of California at San Diego, La Jolla, California 92093-0358

Received August 13, 2004

The reactions of the ligands *N*-methyldiethanol amine and *N*-ethyldiethanol amine (abbreviated H_2mdea and H_2edea, respectively) with $[Mn_{12}O_{12}(O_2CCH_3)_{16}(H_2O)_4]$ yield novel dodecanuclear wheel-shaped products. The capability of the ligands H_2mdea and H_2edea to support wheel structures in metals other than Mn is demonstrated with the crystal structure of a new hexanuclear ferric wheel.

The synthesis of new polynuclear transition metal complexes is driven, in part, by the discovery of single-molecule magnetism.[1] Polynuclear manganese single-molecule magnets (SMMs) are by far the most numerous. The high-spin ground states and resulting slow magnetization dynamics of these SMMs reflect the topological arrangement of the transition metal ions in the molecule. Topological units such as the oxo-centered $[Mn_3O]$ triangle, the $[Mn^{IV}Mn_3^{III}]$ cubane, and the $[Mn_4]$ dicubane are reoccurring structural themes. Wheel-shaped structures occupy a special position among polynuclear compounds for many reasons, not the least of which are the pleasing structural aesthetics.[2] Several recent theoretical studies have indicated that transition metal wheel complexes could be the basis for quantum computation.[3] Many wheel-shaped structures of the first row transition metals are described in a recent review.[4] Wheel-shaped clusters of Mn are rare; the very few examples have only recently been reported. There are three classes of Mn wheel-shaped complexes. The first class consists of metallacrowns since their structure encapsulates hosts. The hexanuclear[5] complex $\{Na\subset[Mn_6]\}^+$ is an example of this type. None of these are SMMs. A second class has polynuclear subunits joined together to form the backbone of the wheel structure. The $[Mn_{22}]$[6] and $[Mn_{84}]$[7] SMMs are composed of repeating $[Mn_4]$ cubane and oxo-centered $[Mn_3O]$ triangular units. A third class incorporates mononuclear units to form the wheel. There are only two reported structures of this type, a $[Mn_6]$[8] and a $[Mn_{10}]$[9] complex, neither of which functions as an SMM. In the present study, the syntheses and magnetic properties of two wheel-shaped $[Mn_{12}]$ complexes belonging to this third class are described. It is shown that both of these $[Mn_{12}]$ wheel complexes are SMMs. Furthermore, a ligand system (Scheme 1) has been identified that gives wheels with Mn and other metals such as Fe.

Scheme 1

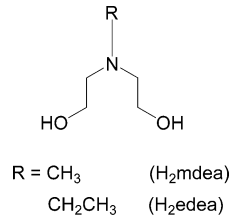

Analytically pure brownish red crystals of $[Mn_{12}(mdea)_8(O_2CCH_3)_{14}]$ (complex **1**) were obtained with the following procedure. To a CH_2Cl_2 (100 mL) slurry of $[Mn_{12}O_{12}(O_2CCH_3)_{16}(H_2O)_4]\cdot 4H_2O\cdot 2CH_3COOH$ (2.0 g, 0.971 mmol) was added dropwise a CH_2Cl_2 (25 mL) solution of H_2mdea (0.462 g, 3.88 mmol). The slurry was allowed to stir overnight, whereupon the Mn_{12} complex slowly dissolved forming a black/brown solution. The undissolved Mn_{12} complex was removed by filtration. The filtrate was evaporated by vacuum distillation yielding a brown oil.

This oil was washed with 30 mL of diethyl ether to remove the excess ligand and then dissolved in 30 mL of acetonitrile and left undisturbed. After 30 min, microcrystals of complex

* To whom correspondence should be addressed. E-mail: dhendrickson@ucsd.edu.

(1) Sessoli, R.; Tsai, H. L.; Schake, A. R.; Wang, S. Y.; Vincent, J. B.; Folting, K.; Gatteschi, D.; Christou, G.; Hendrickson, D. N. *J. Am. Chem. Soc.* **1993**, *115* (5), 1804. Sessoli, R.; Gatteschi, D.; Caneschi, A.; Novak, M. A. *Nature* **1993**, *365* (6442), 141.
(2) Hoffmann, R. *Sci. Am.* **1993**, *268* (2), 66.
(3) Meier, F.; Levy, J.; Loss, D. *Phys. Rev. B* **2003**, *68* (13). Honecker, A.; Meier, F.; Loss, D.; Normand, B. *Eur. Phys. J B* **2002**, 27 (4), 487. Chiolero, A.; Loss, D. *Physica E* **1997**, *1* (1−4), 292. Meier, F.; Loss, D. *Physica B* **2003**, *329*, 1140.
(4) Dolbecq, A.; Secheresse, F. *Adv. Inorg. Chem.* **2002**, *53*, 1.
(5) Abbati, G. L.; Cornia, A.; Fabretti, A. C.; Caneschi, A.; Gatteschi, D. *Inorg. Chem.* **1998**, *37* (7), 1430.
(6) Murugesu, M.; Raftery, J.; Wernsdorfer, W.; Christou, G.; Brechin, E. *Inorg. Chem.* **2004**, *43*, 4203.
(7) Tasiopoulos, A. J.; Vinslava, A.; Wernsdorfer, W.; Abboud, K. A.; Christou, G. *Angew. Chem., Int. Ed.* **2004**, *43* (16), 2117.
(8) Caneschi, A.; Gatteschi, D.; Laugier, J.; Rey, P.; Sessoli, R.; Zanchini, C. *J. Am. Chem. Soc.* **1988**, *110* (9), 2795.
(9) Liu, S. X.; Lin, S.; Lin, B. Z.; Lin, C. C.; Huang, J. Q. *Angew. Chem., Int. Ed.* **2001**, *40* (6), 1084.

10.1021/ic0488886 CCC: $27.50
Published on Web 09/18/2004

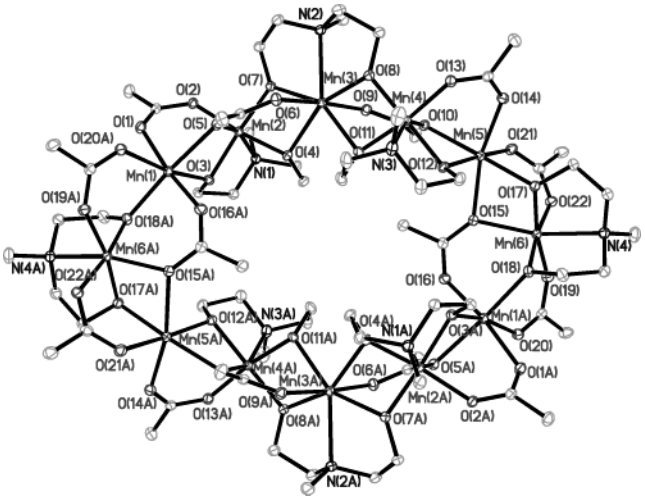

Figure 1. ORTEP of complex **1**, displayed at the 50% probability level. Hydrogen atoms and solvate molecules have been omitted for clarity.

1 started to precipitate. Crystals of the formulation $[Mn_{12}(mdea)_8(O_2CCH_3)_{14}]\cdot CH_3CN$ were grown by allowing diethyl ether vapors to slowly diffuse into an acetonitrile solution of **1**. The same reaction can be used with the H_2eda ligand to give analytically pure crystals of $[Mn_{12}(edea)_8(O_2CCH_3)_{14}]$ (complex **2**).

The tendency of the diethanol amine ligands to give wheel-shaped structures is demonstrated further by the isolation of the hexanuclear ferric wheel, $[Fe_6F_6(edea)_6]$ (complex **3**). To a 70 mL methanol solution of H_2edea (4.96 g, 37.27 mmol) was added a portion of $FeF_3\cdot 3H_2O$ (3.0 g, 17.97 mmol) which did not immediately dissolve. The majority of the FeF_3 dissolved upon heating to reflux yielding a light translucent green solution. The solution was filtered to remove any insoluble matter and then set aside to evaporate. A microcrystalline green sample precipitated the next day. These microcrystals were extremely hygroscopic and analyzed as $[Fe_6F_6(edea)_6]\cdot 10H_2O$. Small green platelet shaped crystals suitable for X-ray diffraction studies were obtained by allowing the solution to slowly evaporate over a period of one week. The compound crystallizes with the formulation $[Fe_6F_6(edea)_6]\cdot 2MeOH\cdot H_2O$.

Figure 1 shows an ORTEP illustration of complex **1**. The crystal structure[10] of **1** consists of six Mn atoms in the asymmetric unit that, along with the other six symmetry related Mn atoms, are arranged in a wheel-shaped topology. The Mn atoms are ligated by acetate and the deprotonated alcohol amine ligand $mdea^{2-}$. These acetate and alkoxide moieties act as bridges between each Mn atom and are the backbone of the wheel. Complex **1** is mixed valent, possessing six Mn(II) and six Mn(III) that alternate around the wheel. The atoms Mn2, Mn4, and Mn6 (and the symmetry related Mn2a, Mn4a, and Mn6a) have been determined to be trivalent by noting their Jahn−Teller distorted geometries.

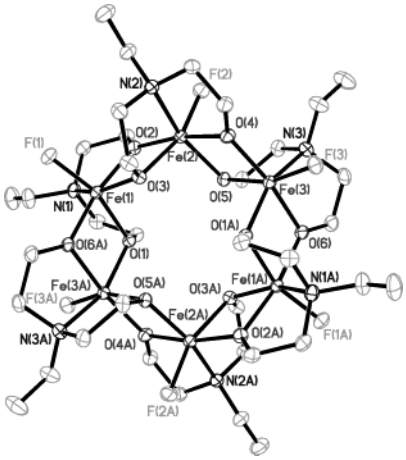

Figure 2. ORTEP of complex **3**, displayed at the 50% probability level. Hydrogen atoms and solvate molecules have been omitted for clarity.

These atoms exhibit Jahn−Teller elongation axes with bond lengths that are significantly longer (e.g., 2.1989(17)−2.311(2) Å for Mn2) than the other bonds (1.8890(17) and 1.9015(17) Å for Mn2). Four of these Jahn−Teller elongation axes (Mn2, Mn2a, Mn4, Mn4a) orient virtually parallel to one another and orthogonal to the plane of the ring. The Jahn−Teller elongation axes of Mn6 and Mn6a orient in the plane of the ring. The atoms Mn1, Mn3, and Mn5, and the symmetry equivalent Mn1a, Mn3a, and Mn5a, are divalent, having bond lengths spanning a much more restricted range (e.g., 2.0972(18) and 2.2502(18) Å for Mn5). The divalent atoms Mn3 and Mn3A are seven-coordinate.

Figure 2 gives an ORTEP illustration[11] of complex **3**. There are three Fe(III) atoms in the asymmetric unit which, along with their other three symmetry related Fe(III) atoms, complete the neutral hexanuclear wheel. Each Fe atom has one fluoride atom and one fully deprotonated $edea^{2-}$ coordinated to it. The μ_2-alkoxide arms of the $edea^{2-}$ ligand bridge each Fe atom with its neighbor. The structure is similar to a related compound[12] in which the fluoride atoms have been replaced with chloride. Compound **3** crystallizes with one water and two methanol molecules of solvation.

Figure 3 illustrates the variable-temperature magnetic susceptibility data for complex **1** measured from 300 K down to 2 K with an applied field of 1 T. The $\chi_M T$ value of 39.7 $cm^3\cdot K\cdot mol^{-1}$ at 300 K is smaller than the theoretical spin-only value of 44.26 $cm^3\cdot K\cdot mol^{-1}$ for six Mn(II) and six Mn(III) noninteracting ions. The value of the product $\chi_M T$ slowly diminishes with decreasing temperature indicating weak antiferromagnetic magnetic exchange interactions. Complex **2** exhibits a similar response.

In order to determine the spin-ground states of complexes **1** and **2**, variable-field magnetization data were collected over several fields down to the lowest temperature of 1.8 K and are depicted in Figure 4. Nonsuperimposable isofields are

(10) Crystal data for **1**: $C_{72}H_{136}N_{10}O_{44}Mn_{12}$, fw = 2505.18, T = 100(2)K; triclinic, space group $P\bar{1}$, a = 13.1038(17) Å, b = 13.2726(18) Å, c = 17.265(2) Å, α = 107.290(2)°, β = 109.195(2)°, γ = 99.309(2)°, V = 2593.1(6) Å^3, Z = 1, D(calc) = 1.604 g cm^{-3}, λ = 0.71073 Å, μ = 14.95 cm^{-1}. For 11460 independent reflections, $R(F)$ = 0.0365 and $R(wF^2)$ = 0.0908.

(11) Crystal data for **3**: $C_{40}H_{98}F_6N_6O_{18}Fe_6$, T = 100(2)K; triclinic, space group $P\bar{1}$, a = 8.6256(14) Å, b = 13.532(2) Å, c = 15.233(2) Å, α = 114.095(2)°, β = 98.170(3)°, γ = 102.634(3)°, V = 1529.4(4) Å^3, Z = 1, D(calc) = 1.520 g cm^{-3}, λ = 0.71073 Å, μ = 14.69 cm^{-1}. For 6878 independent reflections, $R(F)$ = 0.0436 and $R(wF^2)$ = 0.1124.

(12) Saalfrank, R. W.; Bernt, I.; Uller, E.; Hampel, F. *Angew. Chem., Int. Ed. Engl.* **1997**, *36* (22), 2482.

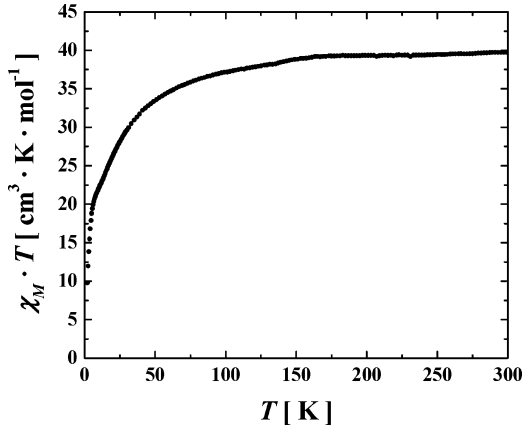

Figure 3. Plot of $\chi_M T$ versus temperature where χ_M is the molar susceptibility for complex **1**. The data were collected with an applied field of 1 T.

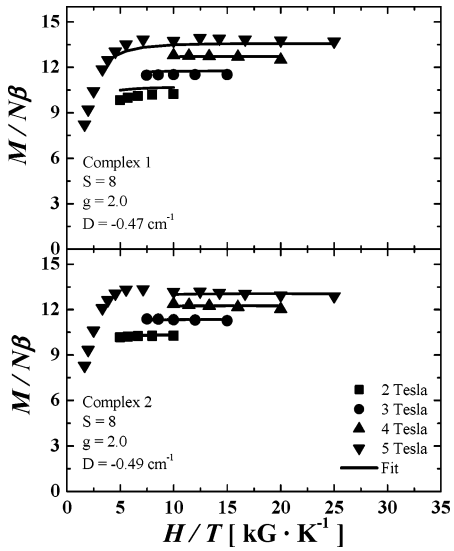

Figure 4. Plot of the reduced magnetization ($M/N\beta$) where M is the molar magnetization, N is Avogadro's number, and β is the Bohr magneton, plotted versus H/T. The solid line represents a least-squares fit of the data. See the text for details.

observed and suggest that complexes **1** and **2** possess significant zero-field splitting in their spin-ground states. Theoretical magnetizations were calculated by means of a full matrix diagonalization (employing a powder average of Gaussian quadrature) of the spin Hamiltonian for an $S = 8$ ground state which included the Zeeman interaction and axial second-order zero field splitting, $D(\hat{S}_z^2)$. These quantities were least-squares fit to the experimental data. A minimum was found with the spin Hamiltonian parameters $S = 8$, $g = 2.0$, and $D = -0.47$ cm^{-1} for complex **1** and $S = 8$, $g = 2.0$, and $D = -0.49$ cm^{-1} for complex **2**. Alternating current magnetic susceptibility data were also collected in the absence of an applied dc field. Figure 5 depicts the temperature dependence of both the in-phase, $\chi'_M T$, and out-of-phase ac susceptibility, χ''_M, collected with several 3 G oscillating ac fields for complex **2**. Figure 5 (upper) displays the in-phase ac susceptibility for complex **2**. The in-phase ac susceptibility data for both complexes **1** and **2** are consistent with the dc susceptibilities (e.g., $\chi'_M T$ (1000 Hz) $= 26.57$ cm^3 K mol^{-1} and $\chi_M T = 22.21$ cm^3 K mol^{-1} at 5 K for complex **2**, and $\chi'_M T$ (1000 Hz) $= 20.71$ cm^3 K mol^{-1}

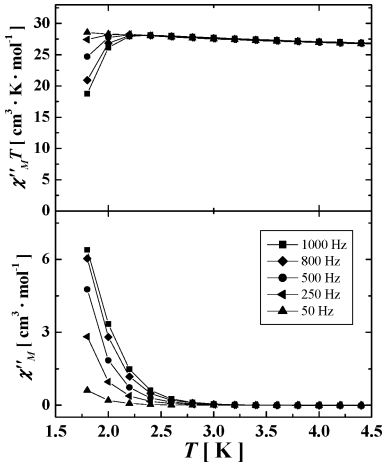

Figure 5. Plot (upper) of $\chi'_M T$ versus temperature where χ'_M is the molar in-phase ac susceptibility for complex **2**. Plot (lower) of χ''_M versus temperature where χ''_M is the molar out-of-phase ac susceptibility for complex **2**.

and $\chi_M T = 18.81$ cm^3 K mol^{-1} at 5 K for complex **1**). The small difference between the dc and ac susceptibilities is due to zero-field splitting effects which would be more pronounced in dc measurements because of the strong applied magnetic field (1 T) at these low temperatures.

It is interesting to note that both complex **2** and complex **1** (not shown) exhibit a frequency dependent out-of-phase component of its ac susceptibility below 2.6 K as seen in Figure 5 (lower). This frequency dependent response indicates that there are slow kinetics of magnetization reversal relative to the frequency of the oscillating ac field and is often associated with the phenomena of single-molecule magnetism.[13] A full peak is not observable in the accessible temperature ranges, with the lowest obtainable temperature being 1.8 K.

Given that both complexes **1** and **2** likely have the high spin-ground state of $S = 8$ and negative magnetic anisotropy as indicated by a zero-field splitting D values of -0.47 cm^{-1} for complex **1** and -0.49 cm^{-1} for complex **2**, it is clear that both complexes are single-molecule magnets. Variable-temperature magnetic susceptibility data collected from 300 K down to 5 K with an applied field of 1 T collected for complex **3** indicate that relatively strong antiferromagnetic interactions lead to an $S = 0$ ground state.

In conclusion, the syntheses and crystal structures of a new [Mn_{12}] complex with a wheel-shaped topology are reported. These new [Mn_{12}] wheel complexes (**1** and **2**) are single-molecule magnets. We are exploring the reactivity of additional diethanol amine ligands with different R-groups (Scheme 1). Low-temperature magnetization measurements are also planned for complexes **1** and **2**.

Acknowledgment. This work was supported by the National Science Foundation.

Supporting Information Available: Crystallographic information files (CIF) for **1** and **3**. This material is available free of charge via the Internet at http://pubs.acs.org.

IC0488886

(13) Christou, G.; Gatteschi, D.; Hendrickson, D. N.; Sessoli, R. *MRS Bull.* **2000**, *25* (11), 66.